# DRIFT SCANNING FROM GROUND AND IN SPACE

M. GAI
*Osservatorio Astronomico di Torino*
*Str. Osservatorio, 20 – I-10025 Pino T.se (TO)*
M.D. GUARNIERI
*European Southern Observatory*
M.G. LATTANZI
*Osservatorio Astronomico di Torino*

(Received 22 November 1996; accepted in final form 25 March 1997)

**Abstract.**
The drift scanning technique offers, in principle, a simple and efficient method for imaging wide regions of the sky with intrinsic high astrometric accuracy. Its performance is analyzed in two distinct environments, namely from a small class ground based telescope and a spaceborne interferometer. In particular, the study is referred to the proposed ESA cornerstone mission GAIA (Global Astrometric Interferometer for Astrophysics).

The constant clock rate of a CCD, due to the declination dependent sidereal speed variation, results in a systematic image smearing, which limits the positional accuracy. Moreover, the readout timing accuracy provides an additional random noise corresponding to a drift speed jitter. Stability requirements on the order of $10^{-6}$ or better have to be fulfilled for the space option.

Both effects can be addressed by proper system design; provisional implementation strategies are discussed for both applications.

## 1. Introduction

A ground based observer can take advantage of the stable rotation of the Earth to measure the distance of objects in the sky: due to their apparent motion, the time elapse between crossing appropriate reference marks provides a position estimate. Such a principle has been widely exploited in the history of transit instruments. With the advent of area detectors, such as the CCDs, the high-accuracy measurement of extended strips of sky became feasible.

On Earth, a drift scanning instrument follows a great circle, pointing onto the plane orthogonal to the rotation axis, only for a specific declination value, i.e. $\delta = 0°$. Besides, a spinning satellite, with its field of view lying on the equatorial plane, intrinsically observes along a great circle; the full sky coverage can be ensured, as in the case of HIPPARCOS (Perryman et al, 1997), through a slow precession of its spin axis. The space environment features both advantages and problems; however, in principle, the limiting accuracy can be much higher than that of ground based instruments.

In perspective, spaceborne surveys bear the promise to push in the near future the positional accuracy to the 10 $\mu$arcsec level; in particular, GAIA is

*Experimental Astronomy* 7: 87-100, 1997.

aimed at a full-sky uniform coverage, including accurate photometric capabilities, up to magnitude V = 15-16. Its scientific scope and baseline design have been extensively revised in a workshop, sponsored by ESA, held at RGO, Cambridge, UK, in June, 1995. For a detailed description, please refer to Lindegren and Perryman (1996), and references therein.

In this framework, the Astronomical Observatory of Torino, involved since the beginning in the preliminary design studies of GAIA, intends to implement a ground based drift scanning camera, with a dual purpose: scientific, aimed at specific activities in the field of galactic population statistics and structure, and technological, in order to develop a test environment for basic techniques related to high accuracy space instrumentation. In particular, the proposed instrument will be used to upgrade the present CCD camera mounted at the OATo 1.05 m astrometric telescope. The project has recently been funded by CRA (Consiglio per le Ricerche Astronomiche, the Italian Astronomical Research Council), and the detailed design is in its completion phase.

In this paper we will discuss both ground based and spaceborne cases, the former to introduce the nomenclature and the concepts in a well known framework, and the latter to analyze them in view of the application to GAIA. The former case study shows that significant scientific results can still be achieved with small telescopes, no longer suitable for many research activities requiring the light gathering power of modern large telescopes. In the latter case, the accuracy potentially achievable would yield impressive scientific results, provided the challenging technological requirements are satisfied by the joint efforts of space engineering, optics, electronics, metrology and other sciences.

The basic mechanism of drift scanning and some parameters of our two reference configurations (namely, a 1 m class ground based telescope and the GAIA interferometer) will be addressed in section 2.

For successively higher declination values, the differential speed over the finite field of view builds up, thus introducing photometric and astrometric errors which shall be discussed in detail in section 3. In the case of GAIA, the offset angle from the great circle is small, but the target accuracy is extremely high, thus the issue deserves to be explicitly addressed.

Drift scanning operates on the assumption of a regular, smooth and known motion (the "scan law"), in order to convert timing information into positional data. Thus, systematic and random errors in the time base are transferred to the target coordinates; this problem is addressed in section 4.

## 2. Drift Scan Applications Framework

The drift scan technique has been used with several variations in different applications, e.g. spectroscopy (Schneider et al., 1994) and low-distortion imaging (Zaritsky et al., 1996). An historical review is beyond the scope of this paper, focused on declination dependent aberrations and timing accuracy requirements.

On Earth, observations at $\delta = 0°$ follow great circles in the sky, whereas a generic declination value introduces an offset towards the equatorial plane. Such an offset modifies most of the observing parameters, and this must be taken in account, both in system design and in subsequent data reduction, in order to achieve the best performance.

One of the error sources is the finite field of view (FOV) of a bidimensional detector, due to the sidereal speed variation with declination. On ground, this limits the potential sky coverage to some declination value identified by the accepted performance degradation.

A spinning satellite, observing in the plane orthogonal to the spin axis, is intrinsically operating along great circles, but, at a very high accuracy level, the offset introduced by the finite size of the field generates a non negligible systematic effect.

Before entering in the evaluation of the aberrations, we will define the case studies of the ground based instrument operated onto a small class telescope and of a spaceborne Fizeau interferometer.

Hereafter, we will refer to the *along scan* direction ($L$) as the ideal path followed by the center of the field of view, roughly corresponding, in ground based drift scanning, with the East-West direction. The orthogonal direction will be labeled as *across scan* or $C$, North-South on ground. We will refer to the ground based configuration as the case (G), and to the spaceborne version as case (S).

### 2.1. Ground: Telescope and Camera Specifications

The OATo astrometric telescope (Reosc, FR, 1.05 m diameter) is equipped since 1993 with a commercial CCD camera (AstroCam, UK). It mounts a detector model CCD05-30 (EEV, UK), and it allows only pointed observations. The upgrade of its electronics, in order to sustain drift scan observations, has just been funded by CRA; delivery (i.e. first observations) is foreseen at end 1997.

The CCD format is 1242 (H) $\times$ 1152 (V), on a pixel size 22.5 $\mu$m (26 $\times$ 28 mm photosensitive area); due to the focal plane optical scale of 20".89/mm, corresponding to an on-chip scale of 0".47/pixel, it provides a (pointed) field of view $\Phi_C = 9'44'' \times \Phi_L = 9'\ 2''$.

In drift scanning mode, the vertical size of the detector corresponds to an exposure time $T_0 = 36\ s$ at $\delta = 0°$ (see below), resulting in an expected limiting magnitude, from present performance figures in pointed mode, $V_{lim} \geq 19$ at $SNR \geq 3$.

### 2.2. Space: the GAIA concept

The GAIA mission has been proposed as an ESA cornerstone mission aimed at high accuracy global astrometry (Lindegren and Perryman, 1994), and the optical concept is well defined (Loiseau and Shaklan, 1995); with respect to the theoretical positional accuracy, an interferometer is competitive with a filled aperture of diameter comparable to the baseline (Lindegren, 1978).

The GAIA optics is a Fizeau interferometer with baseline $B \simeq 2.5$ m and circular apertures of diameter $D \sim 0.5$ m, with an optical scale $\sim 12''/\mathrm{mm}$. The resulting fringe pattern, over a coherent field of view $\Omega \sim 1° \times 1°$, features an Airy disk diameter $\Theta_A \sim 550$ mas and a Young period $\Theta_Y \sim 45$ mas ($\lambda = 550$ nm, $\Delta\lambda = 150$ nm).

The coherent FOV will then occupy $\sim 30 \times 30$ cm, thus it is likely to be implemented by a mosaic of many monolithic detectors.

The system performance assessment, at present, reports uniform sky coverage at the $\sigma \sim 10$ $\mu$arcsec level up to $V = 15 - 16$.

The interferometer spins accordingly to a suitable scan law, with a period $P = 2$ hours, corresponding to a rotational speed $V_G = 180''/s$, and an integration period $T_G = 20\ s$. It covers the whole sky many times, thus providing global positioning onto the celestial sphere through the closure conditions for each great circle and along each orbit during its useful lifetime of 5 years.

#### 2.2.1. *Detection System Options for GAIA*

Different implementations of the detection system have been discussed by Lindegren and Perryman (1995), Høg (1995), and Gai et al. (1995), in the Cambridge '95 Workshop.

The baseline configuration (Lindegren and Perryman, 1995) is based on the use of a modulation grid, as from the HIPPARCOS experience, which builds up a light modulation curve imaged by an array of field lenslets onto a mosaic of CCDs.

Each lenslet corresponds to a subfield of about 30", corresponding to an elementary exposure time $T_i \simeq 0.2$ s. Such subdivision is required to remove source confusion, since the photons from every target in the subfield are superposed.

The subfields also help in reducing the effects of spacecraft noise, since drift speed jitter builds up all along the elementary exposure time $T_i$. The

pointing requirements of GAIA are extremely tight and demand on-board attitude measurement and control (Donati, 1995).

The option of direct imaging of the fringes would allow the suppression of both modulation grid and lenslet array, thus removing a potentially critical element and improving both light economy and astrometric performance (Lindegren, 1978). Imaging requires much higher spatial resolution detectors (Gai et al., 1995). Direct fringe imaging removes the need for division of the FOV, as far as confusion is concerned; however, the attitude problem holds, thus the same limitation on the elementary exposure time has been considered.

Both in the case of the modulation grid and of direct imaging, the most likely detectors are CCDs operated in drift scanning (or time delay integration) mode.

### 2.3. Drift scanning

When orienting a CCD with its columns along the E-W direction, and stopping the telescope tracking, the sidereal motion carries the image of any point in the field of view along the same column(s). Clocking the CCD at the proper rate, the potential wells collecting the photocurrent will move along the device at the same speed of the sky image.

The charge pattern builds up, as in the standard case of pointed observations, all along the transit onto the detector, and the exposure time is proportional to the length of the CCD (i.e. the *along scan* size) and to the drift speed. On ground, the declination-dependent sidereal speed (V) and the exposure time (T) are

$$V = V_0 \cos\delta \qquad V_0 = V(\delta = 0^\circ) \simeq 15"/s$$

$$T = \frac{\Phi_L}{V} = \frac{T_0}{\cos\delta} \qquad T_0 = T(\delta = 0^\circ) = \frac{\Phi_L}{V_0} = 36.1s$$

whereas for GAIA, at the border (B) of its field of view ($\delta_{MAX} = \pm\Phi_C/2 = \pm 30'$, $\Phi_L = 1^\circ$), we have small differences with respect to the nominal values: $V_B = 179.993"/s$ and $T_B = 20.00076\ s$, i.e. a variation of the order $d_B = 1 - \cos\delta_{MAX} = 3.8 \times 10^{-5}$. The elementary integration interval $T_i$ is modified in the same way.

The sidereal speed and exposure time variation with declination are shown in figure 1.

## 3. Declination Dependent Aberrations

The variation of the sidereal speed along the FOV result in field-dependent image distortions, since the charge drift speed over a single CCD is common

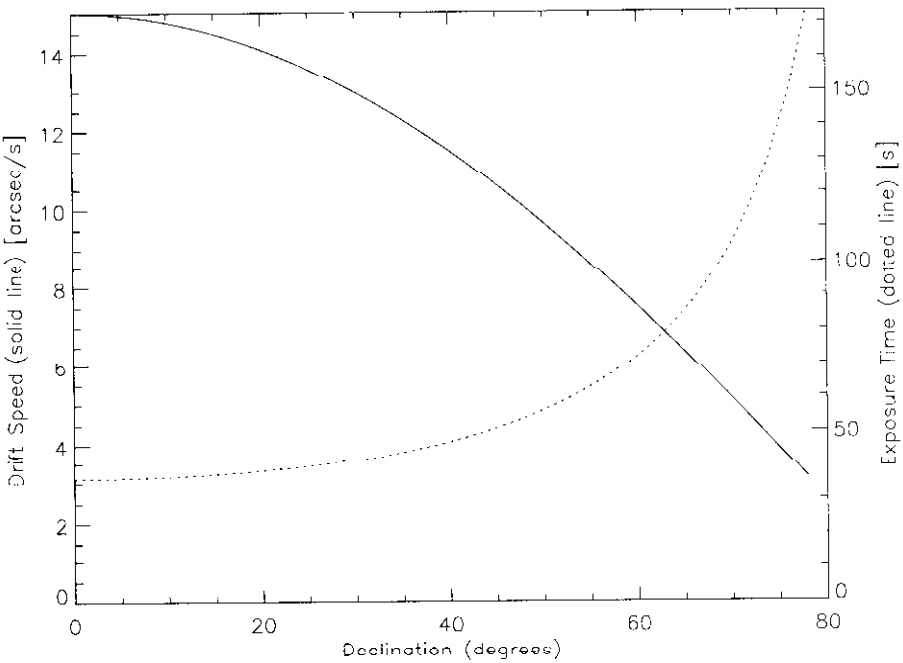


*Figure 1.* Sidereal drift speed and exposure time vs. declination

to the whole device. A perfect matching between them is possible only for a single declination value $\delta_m$. At any displacement $\rho$ with respect to $\delta_m$, the charge pattern suffers a speed error

$$\Delta V = | V(\delta) - V(\delta - \rho) | = 2 V_0 \sin(\delta + \rho/2) \sin(\rho/2)$$

Consequently, the charge distribution, during the elementary exposure period $T_i$ or the transit time $T$, either advances or delays with respect to the instantaneous target image.

The photon image of a point-like source (i.e. the point spread function, PSF) provides photoelectrons which, during the transit, are collected in a position more and more displaced with respect to their correct along scan position. It is a continuous process, resulting in a smearing of the charge image results.

The electronic smearing onto the CCDs can be reduced together with the horizontal (across scan) size of the devices, and increasing their number, at the cost of a corresponding increase in the electronics complexity, because of packaging, wiring, and the large number of output lines.

The computation of the target position must take this effect into account: if the center of mass of the charge distribution is assumed as the correct

centroid, a systematic error is introduced. Besides, this aberration is known: the exact point of matching speed can be identified by analysis of the star shapes along the FOV, then the apparent position shift can be removed with good accuracy. Unfortunately, the charge smearing degrades the signal to noise ratio (SNR) of the aberrated objects, since more pixels contribute their noise to the budget of a given source. Moreover, a confusion problem might arise, for very close targets.

**In case (G),** assuming a transit duration $\sim T$ for both charge and photons, and a speed difference $\Delta V$, the separation (W) between the first and last instantaneous images, which is roughly corresponding to the charge smearing, is

$$W = T \times \Delta V \simeq \rho \, T_0 V_0 \, \tan\delta = \rho \, \Phi_L \, \tan\delta$$

Such effective PSF deformation reaches its maximum at the border of the CCD:

$$W_{MAX} = \frac{1}{2} \, \Phi_C \, \Phi_L \, \tan\delta = 0''.77 \, \tan\delta$$

A sketch of the error in the uncorrected vs. real position of targets along the field and for various declinations is shown in figure 2.

With respect to the scientific performance, reasonably good results can be achieved up to $\delta \sim 60°$; for much higher declination values, something might be gained by an artificial restriction of the FOV, rejecting the data from the borders of the CCD.

Assuming the acceptance of a CCD region of size $\Phi'_C = \Phi_C / \tan\delta$, for $\delta > 60°$, the smearing would be reduced to a constant maximum value $W_{MAX} = \frac{1}{2} \, \Phi_C \, \Phi_L = 0''.77$; the FOV would progressively decrease, reaching 1' size at $\delta = 84°$.

In any case, mosaicing of smaller devices will be mandatory to extend the operability range onto most of the sky with significant efficiency.

**In case (S),** the net effect is a reduction of the electronic fringe pattern *visibility*, with respect to the instantaneous photon distribution, since the dark fringes collect part of the charge which should have been accumulated in the bright areas.

The GAIA focal plane assembly (FPA) is constituted by a mosaic of CCDs, either used for direct imaging or through a modulating grid. Let us assume the case of a $6 \times 6$ array of $\sim 5 \times 5$ cm devices, with each detector strip covering a 10' band in the sky; the drift speed can be selected to match the sidereal speed in the center of each strip, i.e. at $\delta = \pm 5', \pm 15', \pm 25'$. The CCD edges feature a maximum displacement $\rho = 5'$, corresponding to a speed mismatch

$$\Delta V \simeq \rho \, V_G \, (\delta + \rho) = 0.761, \quad 1.141, \quad 1.522 \quad \times 10^{-3} \text{ arcsec/s}$$

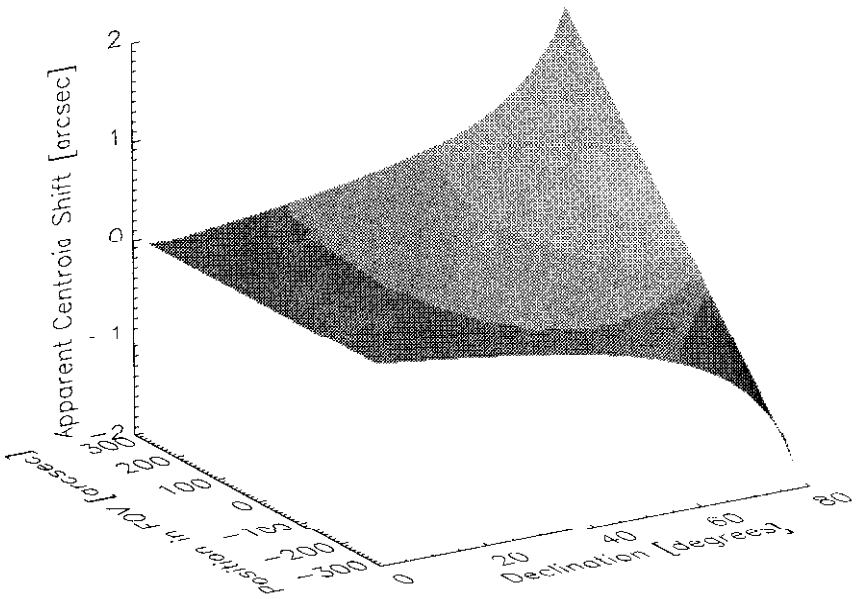


*Figure 2.* Uncorrected centroid position shift in the field vs. declination

resulting into a smearing of the charge image of the fringes, during the elementary exposure time $T_i$,

$$W = T_i \times \Delta V = 152, \quad 228, \quad 304 \ \mu\text{arcsec}$$

corresponding to a relative fringe variation

$$\frac{\Delta\Theta_Y}{\Theta_Y} \simeq \frac{W}{\Theta_Y} = 3.38, \quad 5.07, \quad 6.76 \times 10^{-3}$$

which can be considered as a rough estimate of the fringe visibility variation due to the declination aberrations.

This effect is much smaller than the estimated visibility variation along the FOV (Loiseau and Shaklan, 1995). However, the primary issue of the GAIA detection system is *not* the fringe visibility but its phase, i.e. the position of its centroid. The fringe smearing is deterministic, operating in a specific direction and by a given amount in any point of the FOV. Thus, it can be included in the data reduction as a systematic correction term.

The reduction process provides centroid estimates with an accuracy of a fraction of the fringe period; the exact value depends on the detection

scheme and on the system parameters, and in depth evaluations shall be performed at the proper development stages.

As a first estimate, since the target final accuracy is $\sim$ 10 $\mu$arcsec, and the fringe size is $\sim$ 45 mas, the centroiding "gain" should be $\sim 4.5 \times 10^3$. Assuming that an error compression factor of one order of magnitude arises from the repeated coverage of the sky along the mission lifetime, the single-pass data reduction should provide a maximum centroiding error of $\sim 2 \times 10^{-3}$, corresponding to 90 $\mu$arcsec.

The fringe smearing should feature a similar compression factor, thus introducing a negligible error term in the centroid evaluation: the contribution, mostly deterministic, is less than 1 $\mu$arcsec.

The effect could be further reduced by using smaller CCDs, e.g. a $10 \times 10$ mosaic of 3 cm sized chips, each covering a declination range of 6', with a maximum displacement $\rho = 3'$: at the outer edge of the FOV ($\delta = 27'$), the fringe smearing would be reduced to $\Delta\Theta_Y \simeq 274$ $\mu$arcsec. The packaging and wiring problem can be reduced by integration of several small devices onto a single large silicon die (e.g. two $3 \times 6$ cm CCDs can be placed onto a $6 \times 6$ cm chip). Crosstalk among nearby logical devices onto the same chip, as well as packaging and wiring, are specific issues for future work.

## 4. Timing Requirements for Astrometry

Since the drift scanning mechanism assumes the synchronization of detector operations with the sidereal motion, time base errors result in a degradation of the positional measure, with an effect similar to a drift speed error. We can distinguish between the cases of the clock rate error of a stable time base and of the clock rate fluctuations.

### 4.1. Clock rate offset

In this case, the clock is set to a constant drift speed $V_d$, which does not match the sidereal speed $V_s$ by a small constant offset $V_o$: $V_o = V_d - V_s$. The problem can be identified by its effects; then, previous data can be corrected, whereas the ongoing integration can be tuned to the estimated sidereal speed.

**In case (G),** a small constant error in the mean electronic drift speed has little effect. The whole device is clocked at a rate corresponding to the "mean" sidereal speed, at the center of the device or close to it; the actual sidereal speed is higher on one side and lower on the other. A small clock rate error will then match drift and sidereal speeds at a different, but rather close, point onto the CCD. The net result is a minor performance degradation due to the slightly increased image smearing on one side.

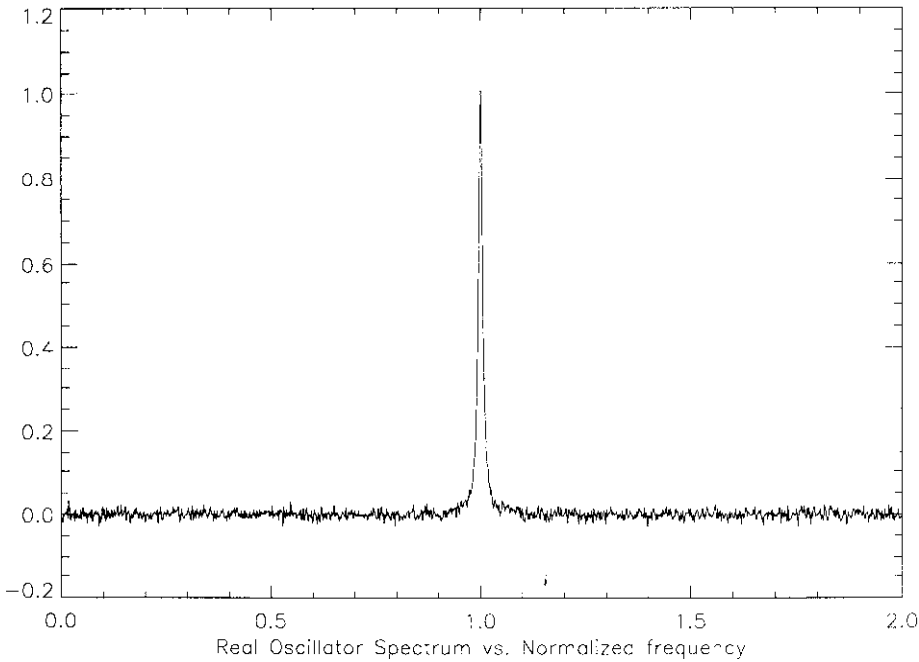


*Figure 3.* Representation of a realistic sinusoidal oscillator spectrum

**In case (S),** the clock rate variation over the field is very small. Thus, the speed error results in a nearly uniform image smearing over the field; in any case, the evaluation of the image quality (i.e. the shape of the fringe pattern) provides a measure of the speed mismatch.

### 4.2. Clock jitter

An ideal sinusoidal oscillator features a Dirac's delta spectrum, operating at a single, stable frequency $\omega_0$. A real-world oscillator, however, has a finite width peak around $\omega_0$, and a noise spectrum distributed over a wide frequency range (see figure 3).

The time base generator of an electronic system provides a square wave with fixed period $\tau_0$, thus an equivalent constant frequency $\omega_0 = 2\pi/\tau_0$ may be defined. The square wave might be generated, for example, by squaring a sine wave by means of a zero-crossing discriminator, thus the above real spectrum problems apply.

The discrete timing of digital electronics, and in particular the CCD clocks, follows the transition edges of the time base waveform, thus events do not happen at the proper fixed rate but suffer (small) random time errors.

Due to the wide spread of the noise spectrum, there are contributions over all time scales; the very low frequency term can usually be identified and corrected, just like the (constant) clock rate offset, as mentioned above. Such slow variation of the device parameters, unfortunately, is also called "drift". The fluctuation of the clock edges with respect to the external time is the so-called jitter, due to the high-frequency components. Intermediate frequency components must be considered with proper care, since in principle they might build up significant error contributions.

An approximate analysis, as shown in basic electronics engineering courses, can be performed on the basis of a global stability figure of the clock rate generator, describing the low to medium frequency terms. In the case of the electronics driving a drift scanning instrument, jitter results in an electronic smearing of the PSF, statistically symmetrical since high frequency terms average to zero, superposed to the systematic image degradation due to declination dependence.

Low-cost crystal oscillators are used in off-the-shelf electronics; they feature a stability $S \sim 10^{-5}$ over the temperature range and during their lifetime, with similar initial accuracy values. Thermal stabilization can improve the stability to $S \sim 10^{-6}$, whereas external trimming and compensation circuits can provide long term regulation (e.g. see ref. Millman Halkias, 1967).

Besides, the desirable long term accuracy can also be achieved by synchronization with an accurate external time base. At the moment, the GPS (Global Positioning System) can easily provide a gain of at least another order of magnitude, reaching a stability $S \sim 10^{-7}$.

Nominal GPS figures report a consistency of 1 $\mu$s with respect to UTC; the dissemination system provides synchronization signals, at 1 s period, with a nominal accuracy of 100 ns (for the PPS version, Precise Positioning System). Thus, the use of GPS receivers, and data time tagging, would result in an external timing error of the order of 1 $\mu$s.

**In case (G),** with a worst-case stability $S \sim 5 \times 10^{-5}$, the cumulative timing error for the whole transit is

$$\Delta T = S \times T = \frac{\Delta T_0}{\cos \delta} \qquad \Delta T_0 = T_0 \times S = 1.8 \text{ ms}$$

The corresponding PSF width enlargement is declination independent:

$$W = \Delta T \times V = \Delta T_0 \times V_0 = 27 \text{ mas}$$

and it is comparable with the astrometric error due to uncorrected atmospheric effects (Lindegren, 1980): 1-2 mas/$\sqrt{hr}$, resulting in 10-20 mas for our case of 36 s transit time. This timing error contributes to the local astrometry budget, i.e. to relative position measures of surrounding stars, over a range comparable with the instantaneous field of view ($\sim 10'$).

For a large telescope equipped with adaptive optics, atmospheric effects are much smaller, and improvements in the instrumental time reference (at least thermal stabilization) might be required.

For wide angle measures, which is the main interest of drift scanning for astrometric purposes, the long-term cumulative effect can become a significant limitation: over a 30° sky strip (2 hours observations at $\delta = 0°$), the timing error (worst case) is $\Delta T = 0.36$ s, i.e. a position error $W = 5.4$ arcsec!

This error corresponds to a smooth geometrical deformation of the image, similar to an optical field distortion; it can be removed by subsequent reduction, for example by matching relevant targets onto a suitable high accuracy catalog. Such catalogs are available: e.g. HIPPARCOS. GPS time tagging is an alternative to the use of a catalog, thus providing a self-consistent instrument, but increasing the implementation complexity beyond the actual necessity; however, it might be an interesting proof-of-concept for future space implementations.

**In case (S),** assuming a good timing stability ($S \sim 10^{-6}$), the charge smearing during an elementary exposure is much smaller than the declination aberration effect:

$$W = V_G \; T_i \; S = 36 \; \mu \text{ arcsec}$$

It is random, not deterministic, and not field dependent; in the GAIA framework, it is a negligible effect.

Since every CCD covering the same sky strip is clocked simultaneously, the *relative* positions of targets in the FOV are preserved, i.e. they suffer the same (small) fringe degradation, but the centroid positions of the charge images are either retained or (slightly) modified in the same way. Moreover, the several device strips may use the same time base, although each is clocked at its proper speed, so that every target in the whole instantaneous coherent FOV of $1° \times 1°$ features the same fringe smearing, without perturbation of the relative position. Since every target is affected in the same way, the effect of timing errors can be identified, e.g. by tracking of bright objects, with high SNR, and/or by statistics over the many objects included in the FOV, but it can not be distinguished from a variation of the instantaneous drift speed. Both timing and drift speed error verification and correction can be included in the first stages of the data processing pipeline; raw data rate estimates suggest that part of the processing might be performed on board, in order to match the telemetry rate, either in analog (Donati, 1995) or digital (Gai et al., 1995) form.

The elementary exposures are not independent, since the time base, in general, features noise components also in the bandwidth corresponding to the time range 0.2-20 s. However, assuming the adoption of an on-board GPS-like reference, the local time base can be reset on a $\sim 1$ s step, thus the timing error can build up between subsequent corrections. Even neglecting

the possibility of correction from smart data analysis, this approach limits the cumulative timing error in 1 s to 180 $\mu$arcsec.

The error of subsequent 1 s steps is uncorrelated, within the internal GPS accuracy (100 ns = 18 $\mu$arcsec), thus the whole transit features a global timing error $180/\sqrt{20} \simeq 40$ $\mu$arcsec, *which is smaller by only a factor 2 than the mentioned target single pass error* 90 $\mu$*arcsec!*

This is *not* negligible, but it is not the best achievable performance. The previous analysis is rather crude, but it provides a result comparable with the design requirements, based on the most elementary application of an established technology. It seems to be likely that the required performance might be achieved with moderate upgrade of currently available timing references and good system engineering.

## 5. Conclusions

Drift scanning offers an extremely simple and elegant method, in principle, for high accuracy positional measurements, both from ground and in space.

On the ground, declination aberrations provide a significant image degradation, but still good astrometric performance over most of the sky; in space, at least for the case of GAIA, the effect is negligible.

The timing stability requirements, on the contrary, are much more stringent in space, due to the much higher targeted accuracy. Besides, current technology specifications are close to such requirements, and some additional developments should suffice to achieve the required performance.

Further studies should allow the definition of a suitable design; at the moment, the electronics requirements seem to be compatible with the state of the art.

## 6. Acknowledgements

We wish to acknowledge CRA for funding the ground based camera.
Documentation on the GPS performance has been obtained on Internet (URL: http://www.utexas.edu/depts/grg/gcraft/notes/gps/gps.html), by the courtesy of Peter H. Dana, The Geographer's Craft Project, Department of Geography, The University of Texas at Austin.

## References

Donati, F.: 1995, 'Attitude Determination and Control for Microarcsec Astrometry', *Future Possibilities for Astrometry in Space*, **ESA SP-379**, pp. 285–287

Gai, M., Lattanzi, M.G., Casertano, S., Guarnieri, M.D.: 1995, 'Non-Conventional Detector Applications for Direct Focal Plane Coverage', *Future Possibilities for Astrometry in Space*, **ESA SP-379**, pp. 231–239

Høg, E.: 1995, 'Some Designs of the GAIA Detector System', *Future Possibilities for Astrometry in Space* **ESA SP-379**, pp. 223–230

Lindegren, L.: 1978, 'Photoelectric Astrometry: A Comparison of Methods for Precise Image Location', F.V. Prochazka and R.H.Tucker (eds.) *Modern Astrometry* **IAU Colloquium n. 48**, pp. 197–215

Lindegren, L.: 1980, 'Athmospheric Limitations of Narrow Field Optical Astrometry', *Astronomy and Astrophysics* **Vol. no. 89**, pp. –

Lindegren, L., Perryman, M.A.C.: 1994, 'GAIA: Global Astrometric Interferometer for Astrophysics (A Concept for an ESA Cornerstone Mission)', *internal report submitted to the ESA Horizon 2000+ Survey Committee*

Lindegren, L., Perryman, M.A.C.: 1995, 'The GAIA Concept', *Future Possibilities for Astrometry in Space* **ESA SP-379**, pp. 23–32

Lindegren, L., Perryman, M.A.C.: 1996, 'GAIA: Global Astrometric Interferometer for Astrophysics', *Astronomy and Astrophysics Supplement Series* **Vol. no. 116**, pp. 579–595

Loiseau, S., Shaklan, S.: 1995, 'Optical Design, Modeling and Tolerancing of a Fizeau Interferometer Dedicated to Astrometry', *Astronomy and Astrophysics Supplement Series* **Vol. no. 117**, pp. 167–178

Millman, J., Halkias, C.C.: 1967, 'Electronic Devices and Circuits', *McGraw-Hill eds.*

Perryman, M.A.C.: 1997, 'The HIPPARCOS Mission', **ESA SP-1200**, in press

Schneider D.P., Schmidt M., Gunn J.E.: 1994, 'Spectroscopic CCD Surveys for Quasars at Large Redshift. III. The Palomar Transit Grism Survey Catalog', *The Astronomical Journal* **Vol. no. 107**, pp. 1245–1269

Zaritsky D., Shectman S.A., Bredthauer G.: 1996, 'The Great Circle Camera: A New Drift-Scanning Instrument', *Publications of the Astronomical Society of the Pacific* **Vol. no. 108**, pp. 104–109

*Address for correspondence:* Osservatorio Astronomico di Torino
Str. Osservatorio, 20 – I-10025 Pino T.se (TO)
e-mail: mario@to.astro.it